Journal of Engineering Physics and Thermophysics, Vol. 77, No. 6, 2004

SIMULATION OF HEAT AND AERODYNAMIC PROCESSES IN REGENERATORS OF CONTINUOUS AND PERIODIC OPERATION. I. NONLINEAR MATHEMATICAL MODEL AND NUMERICAL ALGORITHM

V. P. Kovalevskii

UDC 621.438.536.24

A mathematical model for investigating the processes in regenerator heat exchangers is described. A finite-difference scheme of numerical integration is proposed for solving the conjugate problem on unsteady heat exchange between one-dimensional flows and a two-dimensional matrix wall. The data of test calculations have been compared with the data of other authors. The quasistationary and dynamic processes in a gas-turbine plant regenerator with a matrix of gauzes have been investigated. The optimum design parameters of such a regenerator and rotor speeds providing a maximum heat efficiency of the regenerator at minimum aerodynamic drags in it have been determined.

Introduction. Two types of regenerators — regenerators of continuous and periodic operation — have received the widest acceptance [1, 2]. In a continuous-operation regenerator, a cylindrical or a drum matrix rotates relative to the inlet and outlet pipes with a constant speed, and heat-transfer agents flow through them continuously. A Ljungström regenerator with a rotating matrix and stationary branch pipes and a Rothemühle regenerator with rotating branch pipes and a stationary matrix are typical of this type of regenerator. In a periodic-operation regenerator, the matrix occupies the volume of the body through which the heat-transfer agents are alternately passed. Such a regenerator has a very high heat efficiency. The volume of the regenerator matrix, all things being equal, is much smaller than the volume occupied by the heating surfaces of the recuperative heat exchanger [1–3].

Regenerators are traditionally calculated using linear quasistatic equations with stationary or semi-empirical nonstationary coefficients [1–7]. Such methods and mathematical models [8–13] work well at the initial stages of calculation of the regenerator design.

Numerical mathematical models are usually used for verification and investigation calculations and therefore include relations differing from the above-mentioned equations. For example, in the model developed in [14, 15] the longitudinal heat conduction is taken into account. In the model of [16, 17], the finite value of the transverse heat conduction is considered. In [18], investigations were carried out with account for the finite values of the heat conduction in both directions. The heat accumulated in the flows of heat-transfer agents has been estimated in [19, 20], and a detailed classification of leakages in a regenerator and a method of calculating them have been developed in [21].

The numerical mathematical model developed by us makes it possible to simultaneously take into account the following factors: (1) propagation of heat in the wall of the regenerator matrix in the directions parallel and perpendicular to the flows of heat-transfer agents; (2) distribution of the local heat-transfer coefficients and drag coefficients along the length of the channel; (3) dependence of the thermophysical properties of the heat-transfer agents and the matrix material on the temperature; (4) transport of heat-transfer agents in the matrix and leakages in the packings and in the means for turning the flows; (5) accumulation of heat and mass in the flows of heat-transfer agents; (6) time for which the channels are packed or the time of switching the sections; (7) possibility of using multilayer matrices piecewise-constant in height with straight channels or packings of plates formed to shape, spheres, cylinders, rings, gauzes, or other bodies of various materials. With this model, one can describe the processes occurring in the above-mentioned types of regenerators and in their matrices.

Physical Model. Figure 1 shows diagrams of regenerators of continuous (a, b) and periodic (c) operation. The gas and air, fed to the input of a regenerator, have different pressures and temperatures. Their flow rates are, respec-

President-Neva Energy Center, 4 Zelenogorskaya Str., St. Petersburg, 194156, Russia; email: kovalevskiy@powercity.ru. Translated from Inzhenerno-Fizicheskii Zhurnal, Vol. 77, No. 6, pp. 26–37, November–December, 2004. Original article submitted April 4, 2003; revision submitted January 29, 2004.

 1062-0125/05/7706-1096

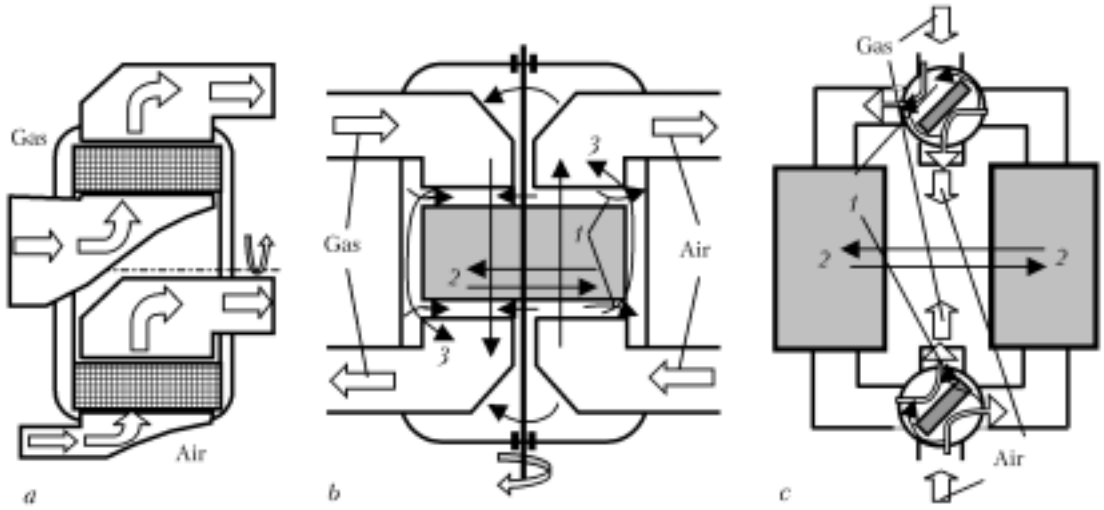

Fig. 1. Diagrams of a continuous-operation regenerator (COR) with a disk (a) and a drum (b) matrix and a periodic-operation generator (POR) (c). Arrows denote the types of possible flows of heat-transfer agents: 1) flow of air to the gas caused by the large difference between their pressures; 2) flows of heat-transfer agents in the channels of the rotating COR matrix and alternating flow of heat-transfer agents in the POR; 3) air and gas flows past the matrix.

tively, $G_{g,in}$ and $G_{a,in}$. The processes in the regenerators considered will be investigated without regard for the second-order factors: (1) end and collector effects in the input and output pipes; (2) difference between the flow sections and the thickness of the matrix channel wall; (3) existence of blocked or defect channels; (4) heat conduction of the matrix material in the circumferential direction; (5) possibility of partial condensation of water vapor in the output cross sections; (6) inertial forces and components of the kinetic and potential energy.

If the processes occurring in parallel radial channels of disk matrices and channels coincident with one and the same generatrix of drum matrices are identical, the operation of any regenerator can be investigated by the example of an individual channel haveng a definite cross section and an arbitrary shape (see Fig. 2a). The outer surface of the channel wall is heat-insulated due to its symmetry. The heat capacity and heat conduction of the wall are determined by the local temperature $\theta(y, z)$, where y is the coordinate coincident with the line measuring the thickness of the matrix wall and z is the coordinate directed along the channel and coincident with the direction of the gas flow.

The gas fed to the input of the channel during a heating cycle of length τ_g has a flow rate $G^1_{g,in}$, a temperature ϑ_{in}, and a pressure $p_{g,in}$. The local coefficient of heat transfer from the gas to the wall α_g and the losses in the pressure $d\Delta p_g$ of the gas that has travelled a distance dz in the channel are determined by the local temperature, pressure, and velocity of the gas. The heat conduction, heat capacity, density, and dynamic (kinematic) viscosity are also determined by the current parameters of the gas. As the heating time τ_g passes, the gas in the channel does not move for the time τ_p. The time τ_p is the time for which the channel is packed (in a continuous-operation generator) or the time for which the valves are turned in a periodic-operation regenerator. The gas and channel-wall temperatures equalize for this time.

As the time $\tau_g + \tau_p$ passes, the air with input parameters $G^1_{a,in}$, t_{in}, and $p_{a,in}$ and parameters distributed along the channel α_a, λ_a, c_{pa}, and ρ_a moves in the channel in the direction opposite to the gas-flow direction during the cooling cycle τ_a. The channel wall cools and gives up its heat to the air. At the instant of time $\tau_g + \tau_p + \tau_a$, the air ceases to move and the channel becomes packed once again for the time τ_p. After the cycle (revolution) with a period $\tau_c = \tau_g + \tau_p + \tau_a + \tau_p$ is completed, the process is repeated from its initial stage.

Mathematical Model. The above-described processes in a regenerator-matrix channel can be defined by the system of energy- and mass-conservation equations for the gas and air flowing in it and the heat-conduction equation for the matrix, including the corresponding initial, boundary, and conjugation conditions and closing relations.

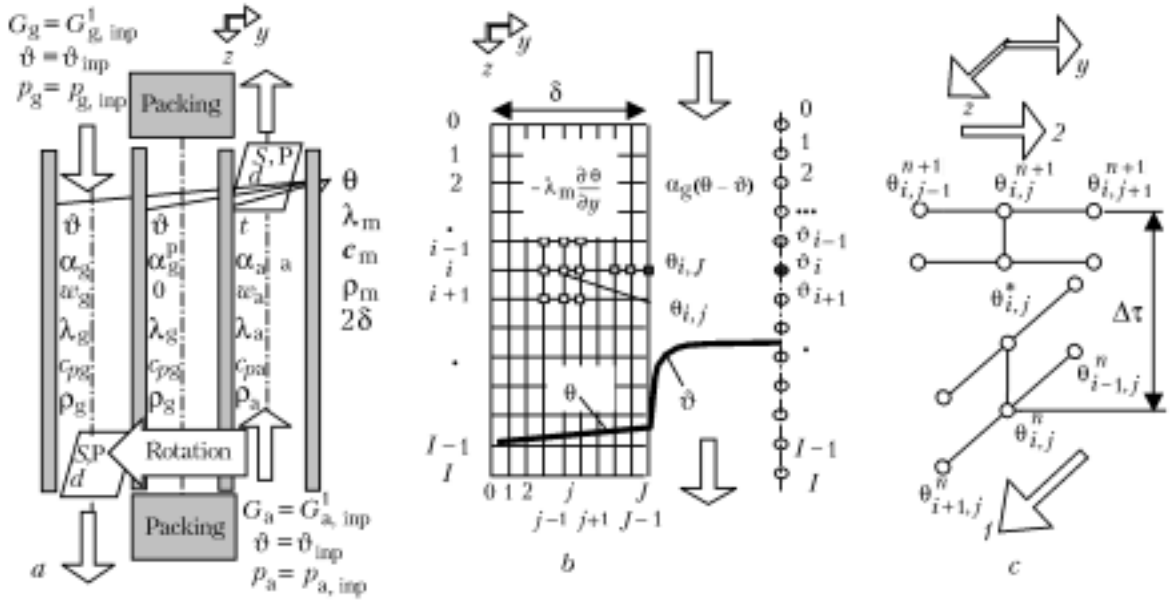

Fig. 2. Elementary channels (a) (arrows denote the directions of the gas and air flows), example of a grid region of integration (b) over the matrix wall for a gas flow (the enumeration of the points i = 0, 1, ..., I along the length of the channel is given in the left part of the figure, the enumeration of the points j = 0, 1, ..., J along the calculated thickness is given in the bottom part) and an air flow (the enumeration of the points i = 0, 1, ..., I along the length of the channel is given in the right part of the figure), and a pattern of integration (c) of the two-dimensional heat-conduction equation by the locally two-dimensional method: 1) direction of the first run-through; 2) direction of the second run-through.

The energy- and mass-conservation equations for the gas and air flowing in opposite directions in a channel of N sections piecewise-constant in geometry for the time τ_c are as follows:

at $0 < \tau \le \tau_g + \tau_p$:

$$S_l c_{vg} \frac{\partial \rho_g \vartheta}{\partial \tau} + \frac{\partial G_g c_{pg} \vartheta}{\partial z} = \Pi_l q_g , \tag{1}$$

$$S_l \frac{\partial \rho_g}{\partial \tau} + \frac{\partial G_g}{\partial z} = 0 , \tag{2}$$

$$q_g = q_{b,g} + n \left\{ \alpha_g [\theta_b - \vartheta] + \varepsilon_{r,g} [\theta_{abs,b}^4 - \vartheta_{abs}^4] \right\} ; \tag{3}$$

at $\tau_g + \tau_p < \tau \le \tau_c$:

$$S_l c_{va} \frac{\partial \rho_a t}{\partial \tau} + \frac{\partial G_a c_{pa} t}{\partial (L - z)} = \Pi_l q_a , \tag{1'}$$

$$S_l \frac{\partial \rho_a}{\partial \tau} + \frac{\partial G_a}{\partial (L - z)} = 0 , \qquad (2')$$

$$q_a = q_{b,a} + n \left\{ \alpha_a [\theta_b - t] + \varepsilon_{r,a} [\theta^4_{abs,b} - t^4_{abs}] \right\} ; \qquad (3')$$

$$l = 1, 2, ..., N .$$

Expressions (3) and (3′) for the specific heat flow q at mixed boundary conditions of the second, third, and fourth order on the outer surfaces will be used hereafter for formulation of the boundary conditions for the heat-conduction equation. Here, n is the projection of a unit vector normal to the boundary surface considered, q_b is the projection of the boundary heat-flow vector (at the second-order condition) whose positive direction coincides with the coordinate-axis direction, and $\varepsilon_r = \varepsilon_b \sigma_0$ is the reduced degree of blackness.

The nonstationary two-dimensional distribution of heat over the N layers of the channel wall in the z direction is defined, in the general case, by the heat-conduction equation

$$c_{lm}(\theta)\, \rho_{lm} \frac{\partial \theta}{\partial \tau} = \sum_{\pi=-1}^{2} b_\pi \frac{\partial}{\partial x_\pi} \left(\lambda_{lm}(\theta)\, k_\pi \frac{\partial \theta}{\partial x_\pi} \right), \qquad (4)$$

where l is the index of the layer considered (l = 1, 2, ..., N) and π is the index of one of the two possible axes of the computational coordinate system, equal to

$$\pi = \begin{cases} -1 & \text{— for the angle coordinate } \varphi \text{ in the polar, cylindrical, and spherical coordinate systems} \\ & \text{in the calculation along the current radius } r^*; \\ 0 & \text{— for all the axes in the Cartesian coordinate system and for the longitudinal azis } z \\ & \text{in the cylindrical coordinate system;} \\ 1 & \text{— for the radial axis } r \text{ in the cylindrical coordinate system;} \\ 2 & \text{— for the radial axis } r \text{ in the spherical coordinate system.} \end{cases}$$

In accordance with the π index introduced, the generalized coordinate x_π and the coefficients of the equation k_π and b_π have the form

$$x_\pi = \begin{cases} \varphi & \text{at } \pi = -1 , \\ z & \text{at } \pi = 0 , \\ r & \text{at } \pi \geq 1 ; \end{cases} \quad k_\pi = \begin{cases} r^{*\pi} & \text{at } \pi = -1 , \\ r^\pi & \text{at } \pi \geq 0 ; \end{cases} \quad b_\pi = \begin{cases} 1/r^* & \text{at } \pi = -1 , \\ 1/k_\pi & \text{at } \pi \geq 0 . \end{cases}$$

Equations (4) are written in Cartesian or cylindrical ($y = r$) coordinates if the case in point is a process in a matrix with straight channels, or in cylindrical or spherical coordinates ($y = r$) for a matrix with a packing. In the first case, the region of integration of the heat-conduction equation is a rectangle (see Fig. 2b) with a width equal to one-half the thickness of the wall and a height equal to the height of the matrix (the length of the channel). In the second case, this region consists of a sequence of subregions, namely, individual cylinders or spheres.

The intensity of the local heat exchange between the gas (air) and the wall is determined by the heat flow, defined by (3) and (3′) and appearing on the right side of energy equations (1) and (1′) as the term q and, in the heat-conduction equation (4), as the mixed boundary conditions on the inner surface of the channel or on the surface of the cylinders or spheres

$$-\lambda_m(\theta) \left. \frac{\partial \theta}{\partial y} \right|_{y=\delta} = q . \qquad (5)$$

The influence of the edge effects on the temperature field along the length of the matrix is assumed to be small. Adiabatic boundary conditions are set at the lower and upper boundaries of the region (ends of the matrix), at the middle point of the matrix wall thickness, or at the axis of the cylinders and spheres (elements of a packing). Let us write them relative to the corresponding normal n:

$$-\lambda_{\mathrm{m}}(\theta)\left.\frac{\partial\theta}{\partial n}\right|_{z=0,L;y=0} = q_{\mathrm{b}} = 0 . \tag{6}$$

The system of equations (1)–(4) is closed, in addition to conjugation conditions (5) and the conditions at the outer boundaries (6), by the following equations:

on the ideal contact surface of the matrix material layers:

$$\lambda_{l\mathrm{m}}(\theta)\left.\frac{\partial\theta}{\partial z}\right|_{z=z_l^{\mathrm{end}}} = \lambda_{l+1,\mathrm{m}}(\theta)\left.\frac{\partial\theta}{\partial z}\right|_{z=z_{l+1}^{\mathrm{in}}}, \quad l = 1, 2, ..., N-1 ; \tag{7}$$

for the local coefficients of heat-transfer between the gas (air) and the wall:

$$\alpha = \alpha\ (\mathrm{Nu}, \mathrm{Gz}, z/d, \text{cross–section shape } S) ; \tag{8}$$

for the states of heat-transfer agents:

$$\rho_{\mathrm{g}} = \rho_{\mathrm{g}}(p_{\mathrm{g}}, \vartheta), \quad \rho_{\mathrm{a}} = \rho_{\mathrm{a}}(p_{\mathrm{a}}, t) ; \tag{9}$$

for the thermophysical properties of the matrix:

$$c_{\mathrm{m}} = c_{\mathrm{m}}(\theta), \quad \lambda_{\mathrm{m}} = \lambda_{\mathrm{m}}(\theta), \quad \rho_{\mathrm{m}} = \rho_{\mathrm{m}}(\theta) ; \tag{10}$$

for the thermophysical properties of the heat-transfer agents:

$$c_{p\mathrm{g}} = c_{p\mathrm{g}}(\vartheta), \quad \lambda_{\mathrm{g}} = \lambda_{\mathrm{g}}(\vartheta), \quad \mu_{\mathrm{g}} = \mu_{\mathrm{g}}(\vartheta) ; \tag{11}$$

$$c_{p\mathrm{a}} = c_{p\mathrm{a}}(t), \quad \lambda_{\mathrm{a}} = \lambda_{\mathrm{a}}(t), \quad \mu_{\mathrm{a}} = \mu_{\mathrm{a}}(t), \quad c_v = c_p - R . \tag{12}$$

The local values of the heat-transfer coefficient are calculated with allowance for the shape of the cross section of the channel or the type and dimension of the packing by the dependences [1, 2, 5, 22, 23] for the laminar, transient, and turbulent regimes of flow at the initial stage of formation of the temperature profile and at the stage of completely developed flow at a constant temperature.

The aerodynamic drag is determined by the generalized distribution of the coefficient of friction $\zeta = \lambda_{\mathrm{f}}\Delta z/d + \zeta_{\mathrm{l.d}}$ (accounting for the friction, the local drag, and the acceleration of the flow) over the length of the channel [2, 5, 22–24].

In the case of a quasistationary regime of flow, the initial conditions for the system of equations (1)–(4) are formulated in the form of an approximate function of the z coordinate and are verified at the end of each characteristic cycle. When the process of heating from the cold state is calculated, initial conditions are assumed to be constant:

for the energy- and mass-conservation equations

$$\begin{gathered} G_{\mathrm{g}}(0, z) = G_{\mathrm{g,in.c}}, \quad p_{\mathrm{g}}(0, z) = p_{\mathrm{g,in.c}}, \quad \vartheta(0, z) = \vartheta_{\mathrm{in.c}} ; \\ G_{\mathrm{a}}(0, z) = G_{\mathrm{a,in.c}}, \quad p_{\mathrm{a}}(0, z) = p_{\mathrm{a,in.c}}, \quad t(0, z) = t_{\mathrm{in.c}} ; \end{gathered} \tag{13}$$

for the heat-conduction equation

$$\theta\,(0, y, z) = \theta_{\text{in.c}}\,. \tag{14}$$

The boundary conditions are as follows:

$$\begin{gathered} G_{\text{g}}\big|_{z=0} = G^1_{\text{g,inp}}\,,\quad p_{\text{g}}\big|_{z=0} = p_{\text{g,inp}}\,,\quad \vartheta\big|_{z=0} = \vartheta_{\text{inp}} - \text{for the gas}\,; \\ G_{\text{a}}\big|_{z=L} = G^1_{\text{a,inp}}\,,\quad p_{\text{a}}\big|_{z=L} = p_{\text{a,inp}}\,,\quad t\big|_{z=L} = t_{\text{inp}} - \text{for the air}\,. \end{gathered} \tag{15}$$

Here $G^1_{\text{g,inp}}$ ($G^1_{\text{a,inp}}$) is the rate of the heat-transfer agent flow per elementary channel of the gas (air) sector. The prescription of the flow rate at the input of the channel is only conditionally correct.

In accordance with the mathematical model, the temperature at the output of an individual channel and the pressure drop along its length will constantly change. This is true for a periodic-operation regenerator. To determine the temperature at the output of a continuous-operation regenerator, it is necessary to calculate the average integral temperature of a heat-transfer agent at the output of an individual channel. The integration procedure is as follows:

$$\begin{gathered} \bar{\vartheta}_{\text{out}} = \left[\int_0^{\tau_{\text{g}}} (Gc_p\vartheta)_{\text{g,out}}\,(\tau)\,d\tau\right] \Big/ \left[\int_0^{\tau_{\text{g}}} (Gc_p)_{\text{g,out}}\,(\tau)\,d\tau\right], \\ \bar{t}_{\text{out}} = \left[\int_{\tau_{\text{g}}+\tau_{\text{p}}}^{\tau_{\text{g}}+\tau_{\text{p}}+\tau_{\text{a}}} (Gc_p t)_{\text{a,out}}\,(\tau)\,d\tau\right] \Big/ \left[\int_{\tau_{\text{g}}+\tau_{\text{p}}}^{\tau_{\text{g}}+\tau_{\text{p}}+\tau_{\text{a}}} (Gc_p)_{\text{a,out}}\,(\tau)\,d\tau\right]. \end{gathered} \tag{16}$$

Physically this means that flows of each heat-transfer agent in all the channels are mixed in the output pipe at a definite instant of time. The pressure drops in the gas Δp_{g} and air Δp_{a} paths of the matrix are determined analogously:

$$\bar{\Delta}p_{\text{g}} = \frac{1}{\tau_{\text{g}}}\int_0^{\tau_{\text{g}}} \Delta p_{\text{ch,g}}\,(\tau)\,d\tau\,,\quad \bar{\Delta}p_{\text{a}} = \frac{1}{\tau_{\text{a}}}\int_{\tau_{\text{g}}+\tau_{\text{p}}}^{\tau_{\text{g}}+\tau_{\text{p}}+\tau_{\text{a}}} \Delta p_{\text{ch,a}}\,(\tau)\,d\tau\,. \tag{16′}$$

The efficiency of the regenerator was determined with account for the temperature dependence of the heat capacity, the change in the rates of flows in the packings, and the mass transfer in the matrix channels from the equations for η_{g} and η_{a} (the quantities η_{g} and η_{a} are not equal in the general case):

$$\eta_{\text{g}} = \frac{Q_{\text{g}}}{Q_{\text{g}}^{\max}} = \frac{(G_{\text{g}}c_{p\text{g}}\vartheta)_{\text{av,inp}} - (G_{\text{g}}c_{p\text{g}}\vartheta)_{\text{av,out}}}{(G_{\text{g}}c_{p\text{g}}\vartheta)_{\text{av,inp}} - (G_{\text{g}}c_{p\text{g}}t)_{\text{av,inp}}}\,,\quad \eta_{\text{a}} = \frac{Q_{\text{a}}}{Q_{\text{a}}^{\max}} = \frac{(G_{\text{a}}c_{p\text{a}}t)_{\text{av,out}} - (G_{\text{a}}c_{p\text{a}}t)_{\text{av,inp}}}{(G_{\text{a}}c_{p\text{a}}\vartheta)_{\text{av,inp}} - (G_{\text{a}}c_{p\text{a}}t)_{\text{av,inp}}}\,. \tag{17}$$

Computational Algorithm. The system of equations (1)–(17) entering into the mathematical model is solved by the finite-difference method [25, 26]. All the equations are approximated using the grids presented in Fig. 2b and c, which are uniform within the matrix-material layer, one-dimensional in the z direction for flows, and two-dimensional for the heat-conduction equation.

Finite-Difference Scheme for Solving the Heat-Conduction Equation. The two-dimensional heat-conduction equation is solved using the locally one-dimensional method [26, 27] by repeated, successive solving one-dimensional equations (see Fig. 2b and c). Below are finite-difference analogs of the nonlinear, one-dimensional heat-conduction equation (4), obtained by the integro-interpolation method described in [25]. Hereinafter the expressions are written with the following notation (see Fig. 2b and c): n and $n+1$, previous and current time layers (n = 0, 1, 2, ...), the index $n+1$ will be frequently omitted for brevity; $\theta_i = \theta_i^{n+1}$ ($i = m-1$, m, and $m+1$ are used for the temperatures at adjacent points and m = 1, 2, ..., $M-1$; $i = m-1/2$ and $m+1/2$ are used for the temperatures and coefficients averaged over the integration region); σ_τ, Crank–Nicholson approximation parameter (σ_τ = 1.0 for implicit schemes and

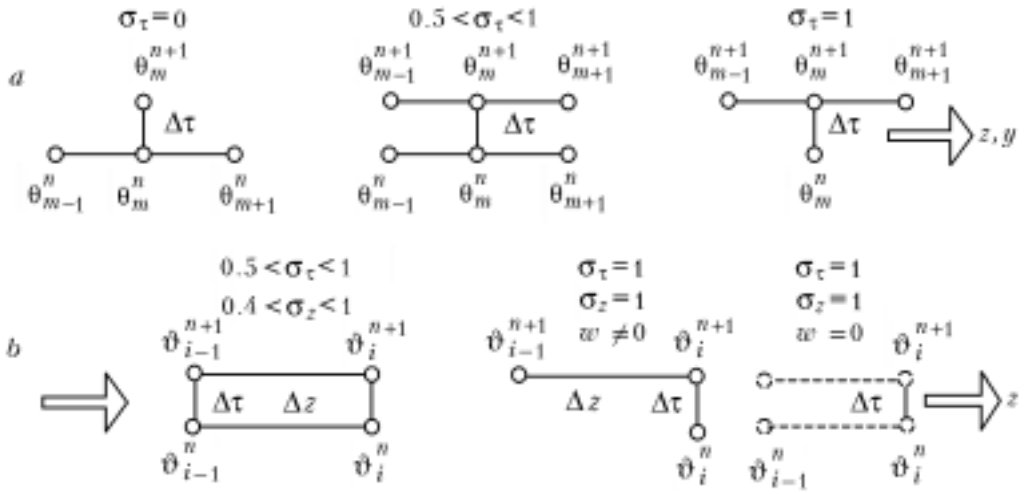

Fig. 3. Patterns of the finite-difference scheme for the one-dimensional heat-conduction equation (a) and the equation of energy and mass conservation for the flows of heat-transfer agents (b).

σ_τ = 0.5 for schemes of the second order of accuracy with respect to $\Delta\tau$). Patterns of the finite-difference schemes used for solving the heat-conduction equation are presented in Fig. 3a. For brevity of representation of expressions, we will omit the index π for x and b and the index l for the thermophysical properties of each of the layers.

On introduction of the notations

$$\sigma_\tau^- = 1 - \sigma_\tau\,,\quad x_m^\pm = x_{m\pm1/2} = x_m \pm 0.5h_m^\pm\,,\quad k_m^\pm = (x_m^\pm)^\pi\,;\quad \gamma_m^\pm = k_m^\pm\lambda\,(\theta_{m\pm1/2}^n)\,;\quad d_m = d_m^- + d_m^+\,;$$

$$d_m^\pm = c^\pm\,(\theta_m^n)\,\rho_m^\pm h_m^\pm/(2b_m\Delta\tau)\,;\quad a_m^\pm = \gamma_m^\pm/h_m^\pm\,;\quad \beta_m^\pm = \sigma_\tau a_m^\pm\,;\quad \beta_m = d_m + \sigma_\tau\,(a_m^- + a_m^+)\,; \tag{18}$$

$$f_m = -\,d_m\theta_m^n - \sigma_\tau^-\,[a_m^-\theta_{m-1}^n - (a_m^- + a_m^+)\,\theta_m^n + a_m^+\theta_{m+1}^n]$$

the finite-difference analog of the heat-conduction equation for the inner regions takes the form of a three-diagonal system of algebraic equations relating the temperatures at three adjacent points:

$$\beta_m^-\theta_{m-1} - \beta_m\theta_m + \beta_m^+\theta_{m+1} = f_m\,,\quad m = 1, 2, ..., M-1\,. \tag{19}$$

Using the equation of heat balance at the left boundary ($n = -1$) and dependence (3) for the heat flow, we obtain an equation relating the temperatures at the zero and first points to the first run-through coefficients E_1 and U_1:

$$\theta_0 = E_1\theta_1 + U_1\,, \tag{20}$$

where

$$E_1 = \beta_0^+/B_0\,;\quad U_1 = (d_0^+\theta_0^n + \sigma_\tau k_0\alpha_{in\Sigma}\,(\tau_{n+1})\,t_{in,b} + C_{in})/B_0\,. \tag{21}$$

In expressions (21)

$$B_0 = d_0^+\beta_0^+ + \sigma_\tau k_0\alpha_{in\Sigma}\,(\tau_{n+1})\,;\quad \alpha_{in\Sigma} = \alpha_{in,b}\,(\tau_{n+1}) + \alpha_{in,beam}\,;$$

$$\alpha_{\text{in,beam}} = \varepsilon_{\text{in,r}} (\theta^n_{\text{abs0}} + t_{\text{abs,in,b}}) [(\theta^n_{\text{abs0}})^2 + (t_{\text{abs,in,b}})^2] ; \quad C_{\text{in}} = \sigma^-_\tau a^+_0 (\theta^n_1 - \theta^n_0) + C_{\text{in,b}} ;$$

$$C_{\text{in,b}} = k_0 \left\{ \sigma_\tau q_{\text{in,b}} (\tau_{n+1}) + \sigma^-_\tau [q_{\text{in,b}} (\tau_n) - \alpha_{\text{in,b}} (\tau_n) ((\theta^n_0 - t^n_{\text{in,b}}) - \varepsilon_{\text{in,r}} (\theta^n_{\text{abs0}})^4 - (t_{\text{abs,in,b}})^4)] \right\} .$$

Assuming that the temperature at the point $m - 1$ is related to the temperature at the point m (the temperatures at the points 0 and 1 are related by (20)) as

$$\theta_{m-1} = E_m \theta_m + U_m \tag{22}$$

and substituting the above relation into (19), we obtain recurrence relations for the run-through coefficients

$$E_{m+1} = -\beta^+_m / B_m ; \quad U_{m+1} = (f_m - \beta^-_m U_m) / B_m ; \quad B_m = \beta^-_m E_m - \beta_m , \tag{23}$$

by which one can successively calculate all the coefficients E_{m+1} and U_{m+1} (m = 1, 2, ..., $M - 1$) and thus determine the relation between θ_{M-1} and θ_M at the end right boundary when the temperatures at the points are unknown.

Using the equation of heat balance at the right boundary (n = 1) and relation (23) for the run-through coefficients E_M and U_M, we can obtain a simple equation relating the temperature at the Mth point θ_M to the heat-transfer agent temperature $t_{\text{end,b}}$:

$$\theta_M = A t_{\text{end,b}} + B . \tag{24}$$

The coefficients A and B are determined from the expressions

$$A = [\sigma_\tau k_M \alpha_{\text{end}\Sigma} (\tau_{n+1})] / C , \quad B = [d^-_M \theta^n_M + \beta^-_M U_M - C_k] / C , \tag{25}$$

where

$$\alpha_{\text{end}\Sigma} (\tau_{n+1}) = \alpha_{\text{end,b}} (\tau_{n+1}) - \varepsilon_{\text{end,r}} (\theta^n_{\text{abs}M} + t^*_{\text{abs,end,b}}) [(\theta^n_{\text{abs}M})^2 + (t_{\text{abs,end,b}})^2] ;$$

$$C = d^-_M + \beta^-_M (1 - E_M) + \sigma_\tau k_M \alpha_{\text{end}\Sigma} (\tau_{n+1}) ; \quad C_{\text{end}} = \sigma^-_\tau a^-_M (\theta^n_M - \theta^n_{M-1}) + C_{\text{end,b}} ;$$

$$C_{\text{end,b}} = k_M \left\{ \sigma_\tau q_{\text{end,b}} (\tau_{n+1}) + \sigma^-_\tau [q_{\text{end,b}} (\tau_n) + \alpha_{\text{end,b}} (\tau_n) (\theta^n_M - t^n_{\text{end,b}}) + \varepsilon_{\text{end,r}} (\theta^n_{\text{abs}M})^4 - (t^n_{\text{abs,end,b}})^4)] \right\} .$$

In what follows, the coefficients A and B will be used in solving the finite-difference analogs of the energy equation of flows.

Thus, we have obtained all the finite-difference analogs of the one-dimensional heat-conduction equation. They are solved in three steps. First (forward run-through), the first run-through coefficients E_1 and U_1 are calculated for m = 0 by formulas (21) at boundary conditions (6) and all the coefficients E_{m+1} and U_{m+1} are successively calculated for m = 1, 2, ..., $M - 1$ by recurrence relations (23). Then the temperature θ_M at the end right boundary is determined. In solving the ordinary problem along the z axis, the temperature θ_M is determined directly from (24) at $t^*_{\text{end,b}} = t_{\text{end,b}}$. In solving the conjugate problem in the direction transverse to the z axis, this temperature is determined after the temperature $t_{\text{end,b}}$ has been found from the energy equation for the gas flow at $t^*_{\text{end,b}} = t^n_{\text{end,b}}$ (see the section below). Finally, the temperature at all the other points is determined from relation (22) for $m = M$, $M - 1$, ..., 1 by backward run-through.

Finite-Difference Analogs of the Energy- and Mass-Conservation Equations. Finite-difference analogs of the energy- and mass-conservation equations (1) and (2) (for the gas) will be constructed by the implicit scheme with weights σ_τ and σ_z ($\sigma^-_z = 1 - \sigma_z$) [26]. For brevity of representation of expressions, we will omit the superscript $n + 1$

for the current time layer and the subscripts *g*, *p*, and *l*. The symbols of operations are repeated in the next line. We obtain (see the patterns in Fig. 3b) the following:

for the energy-conservation equation

$$Sc_{\text{vav}i}\left\{[\sigma_z(\rho\vartheta)_i + \bar{\sigma}_z(\rho\vartheta)_{i-1})] - [\sigma_z(\rho\vartheta)_i^n + \bar{\sigma}_z(\rho\vartheta)_{i-1}^n)]\right\}/\Delta\tau +$$

$$+\left\{\sigma_\tau[(Gc\vartheta)_i - (Gc\vartheta)_{i-1}] + \bar{\sigma}_\tau[(Gc\vartheta)_i^n - (Gc\vartheta)_{i-1}^n]\right\}/\Delta z =$$

$$= \Pi\left\{\sigma_\tau[\sigma_z\alpha_i(\theta_i - \vartheta_i) + \bar{\sigma}_z\alpha_{i-1}(\theta_{i-1} - \vartheta_{i-1})] + \bar{\sigma}_\tau[\sigma_z\alpha_i^n(\theta_i^n - \vartheta_i^n) + \bar{\sigma}_z\alpha_{i-1}^n(\theta_{i-1}^n - \vartheta_{i-1}^n)]\right\}, \quad (26)$$

where the heat capacity averaged over the integration band i is approximated, at a constant volume, as

$$c_{\text{vav}i} = \sigma_\tau(\sigma_z c_i + \bar{\sigma}_z c_{i-1}) + \bar{\sigma}_\tau(\sigma_z c_i^n + \bar{\sigma}_z c_{i-1}^n) - R;$$

for the mass-conservation equation

$$S[(\sigma_z\rho_i + \sigma_z - \rho_{i-1}) - (\sigma_z\rho_i^n + \bar{\sigma}_z\rho_{i-1}^n)]/\Delta\tau + \left\{\sigma_\tau[G_i - G_{i-1}] + \bar{\sigma}_\tau[G_i^n - G_{i-1}^n]\right\}/\Delta z = 0, \quad (27)$$

$$i = 1, 2, ..., I.$$

From here on we will consider only the direction along the flow, i.e., will solve the problem with respect to the current output temperature ϑ_i and the flow rate G_i at the ith point. Rearrangement of Eqs. (26) and (27) with the use of Eq. (24) ($\theta_i = A\vartheta_i + B$) gives:

for the energy-conservation equation

$$\vartheta_i = \left\{S\Delta z c_{\text{vav}i}[\sigma_z(\rho\vartheta)_i^n + \bar{\sigma}_z(\rho\vartheta)_{i-1}^n - \bar{\sigma}_z(\rho\vartheta)_{i-1})] - \left\{\bar{\sigma}_\tau[(Gc\vartheta)_i^n - (Gc\vartheta)_{i-1}^n] - \sigma_\tau(Gc\vartheta)_{i-1}\right\}\Delta\tau +\right.$$

$$+\Pi\Delta z\Delta\tau\left\{\sigma_\tau[\sigma_z\alpha_i B + \bar{\sigma}_z\alpha_{i-1}(\theta_{i-1} - \vartheta_{i-1})] + \bar{\sigma}_\tau[\sigma_z\alpha_i^n(\theta_i^n - \vartheta_i^n) + \bar{\sigma}_z\alpha_{i-1}^n(\theta_{i-1}^n - \vartheta_{i-1}^n)]\right\}/\left\{S\Delta z c_{\text{vav}i}\sigma_z\rho_i +\right.$$

$$\left.\left. + \sigma_\tau\Delta\tau(Gc)_i + \Pi\Delta z\Delta\tau\sigma_\tau\sigma_z\alpha_i(1 - A)\right\}\right.; \quad (28)$$

for the mass-conservation equation

$$G_i = G_{i-1} - \left\{\bar{\sigma}_\tau\Delta\tau[G_i^n - G_{i-1}^n] + S\Delta z[(\sigma_z\rho_i + \bar{\sigma}_z\rho_{i-1}) - (\sigma_z\rho_i^n + \bar{\sigma}_z\rho_{i-1}^n)]\right\}/\sigma_\tau\Delta\tau. \quad (29)$$

Having determined the coefficients A and B by forward run-through of the heat-conduction equation, we may solve these equations for the output temperature ϑ_i and flow rate G_i at all the points i = 1, 2, ..., I at corresponding iteration approximations ϑ_i^* and ρ_i^* prescribed and refined in each integration band.

Let us investigate the limiting cases of relation (28) and verify it. This can be most simply done when this relation is solved by the implicit scheme for the output point, i.e. (see Fig. 3b), at σ_τ = 1, σ_i = 1, and $c_{\text{av}i} = c_i$. It is evident that $\vartheta_i \to \vartheta_i^n$ at very small steps approaching zero ($\Delta\tau \to 0$). At very large steps tending to infinity ($\Delta\tau \to \infty$), corresponding to the case of asymptotic solution, (28) is rearranged into the balance equation

$$\vartheta_i = [(Gc\vartheta)_{i-1} + \Pi\Delta z\,\alpha_i B]/[(Gc)_i + \Pi\Delta z\,\alpha_i(1 - A)]. \quad (30)$$

At flow rates approaching zero and finite (the channel is packed) or very large ($\alpha \to \infty$) heat-transfer coefficients, from Eq. (30) we obtain

TABLE 1. Comparison of the Data of Calculations of the Parameters of Gas-Turbine-Plant Regenerators with Various Matrices by the Program Proposed (right column) with the Analogous Data of Other Authors (left column)

Parameter	Source of data compared							
	[2], pp. 343, 348		[21]		[5], p. 163		[23], p. 320	
Shape of the channel or type of the packing	Spheres		Triangular		Triangular		Gauze	
Dimensions, mm or number of cells per meter of the grid	Diameter 10		Side 0.76		Side 1.58		945×955	
Thickness of the wall, mm	10		0.076/0.082		0.1		0.34	
Material	Granite		Ceramics		Steel		Steel	
Heat conduction, W/(m·K)	2.79		0.19		20—0.029θ		20.0	
Heat capacity, J/(kg·K)	775		1089		500		500	
Density, kg/m^3	2630		2214		800		7817	
Height of the matrix (length of the channel), m	2.0		0.0747		0.1655		0.0212	
Total flow section, m^2	0.2		0.2806		5.701		3.47	
Part of the section occupied by the hot heat-transfer agent/part occupied by the packing	0.5/0.0		0.49/0.05		0.62/0.035		0.715/0.0	
The same for the cold heat-transfer agent	0.5/0.0		0.41/0.05		0.31/0.035		0.285/0.0	
Rotational speed, rpm	0.5		15		15		26.5	
Input gas flow rate, kg/sec	0.1		0.71		40.5		9.6425	
Input gas pressure, Pa	100 000		105 000		103 000		105 000	
Input gas temperature, °C	50		865		425		675	
Input air flow rate, kg/sec	0.1		0.70		40.5		9.5	
Input air pressure, Pa	100 000		393 000		497 000		329 000	
Input air temperature, °C	50		204		215		168	
Matrix porosity, %	0.4	0.4	0.710	0.710	—	0.812	0.725	0.725
Surface in 1 m^3 of the volume, m^2/m^3		360	6460	6466	—	3561	3215	3235
Heat-exchange surface, m^2	—	144	—	135.6	4180	4137	238	238
Matrix material mass (working), kg	—	631.2	—	13.5	1672	1746	159	158
Heat output, kW	—	0	—	475.7	6658	7025	—	4204
Output gas temperature, °C	50	50	266.4	259.1	270	274	244	280
Mean heat-transfer coefficient of the gas, W/(m^2·K)	100.2	102.0	—	419.1	187	177	687	707
Drag to the gas, kPa	3230	3216	6641	6827	3210	3112	1754	2006
Output air temperature, °C	50	50	824.4	825.1	372	381	598	584
Mean heat-transfer coefficient of the air, W/(m^2·K)	100.2	103.4	—	406.9	161	167	1050	1077
Drag to the air, kPa	3230	3219	1950	1990	1320	1310	2273	2233
Efficiency by the temperature, %	—	—	0.938	0.940	0.748	0.790	0.820	0.924
Efficiency by the heat balance, %	—	—	—	0.936	—	0.787	—	0.824
Calculated number of complete cycles	—	22	—	48	—	40	—	30
Heat imbalance in the finite cycle, %	—	—	—	–0.12	—	0.021	5.5	–0.02

Note. As in other works, the calculations were carried out without regard for the leakages and flows of heat-transfer agents in the matrix.

[2], isothermal blow through the spheres packed in a random way; the conditional heating cycle was calculated by the thermophysical properties determined by the authors, and the corresponding cooling cycle was calculated by the program.

[21], air was used as a heat-transfer agent, since a ratio between the heat capacities of the heat transfer agents of 1.02 was used by the authors and the air excess was not indicated; the thickness of the wall was corrected to the coincidence with respect to the porosity.

[5], the thermophysical properties were calculated because the authors did not present data on the air excess, and the air heat capacity estimated by the heat balance was equal to 1047.

[23], the calculated model is a gauze packing of wires with heat-insulated ends; the heat imbalance was estimated by the data of the authors and was 5.5%.

$$\vartheta_i = B/(1-A) = \theta_i\,, \tag{31}$$

since, at $\theta_i = \vartheta_i$, relation (24) ($\theta_i = A\vartheta_i + B$) takes the form

$$\vartheta_i = A\vartheta_i + B\,, \quad \text{or} \quad \vartheta_i\,(1-A) = B\,, \quad \text{or} \quad \vartheta_i = B/(1-A)\,. \tag{32}$$

The temperatures at the adjacent points of the flow ϑ_i and the wall θ_i tend, according to (31), to equalize. Consequently, Eq. (28) can be used for calculation of a packed channel in which the rate of flows is zero.

In the case of nonzero flow rates, Eq. (30) takes the form

$$(Gc\vartheta)_i - (Gc\vartheta)_{i-1} = \Pi\,\Delta z\,\alpha_i\,[B - (1-A)\,\vartheta_i] = \Pi\,\Delta z\,\alpha_i\,[\theta_i - \vartheta_i]\,. \tag{33}$$

This is an ordinary balance equation in which heat accumulation is not taken into account. It is this form of equation (28) (at $\Delta\tau \to \infty$) that allows one to fairly accurately estimate the initial temperature (and pressure) (13) of the heating and cooling cycles under quasistatic operating conditions.

Algorithm for Solving the Conjugate Problem. It is proposed to solve the system of equations of the conjugate problem by a modified method of run-through in conjugate directions [28]. Below is a description of this method.

For a matrix with straight channels, we will perform forward and backward run-through along the z coordinate for all the layers j = 0, 1, 2, ..., J forming its thickness. When conditions (6) are set at the ends of the matrix, this run-through is not related to the flows of heat-transfer agents. The intermediate temperature field obtained is not a physical solution. This operation will be omitted for matrices packed with particles.

Then we will perform forward run-through along the y coordinate, which is perpendicular to the gas flow, from the zero point at the heat-insulated boundary to the δ point at the channel wall around which the gas flows. At the above-indicated boundary conditions (with the difference that, in the input cross section, i = 0 for the gas and i = I for the air), backward run-through begins with determination of the temperature at the end point (i, J) of the wall by formula (24). As for the other points i, this formula only relates the wall temperature $\theta_{i,J}$ to the gas temperature ϑ_i. In combination with energy equation (26), we have two equations for determining these two unknown temperatures. Thus, the temperature of the flow at the output point ϑ_i (relation (28)) and the temperature at the boundary point of the matrix $\theta_{i,J}$ (relation (24)) can be determined. Thereafter, by backward run-through of (22) in the y direction, we determine the inner temperatures of the wall $\theta_{i,J}$ at all the ith points of the grid.

Then we may pass to the next (in the direction of the gas flow) grid layer $i+1$. Determination of the temperatures of the gas and the matrix wall in the time layer $n+1$ at all the points of the grid completes the calculation at the current time step $\Delta\tau$. These temperature fields represent a physical solution. After the parameters of the $(n+1)$th layer are given to the nth layer, one may pass to the calculation at the next time step. This algorithm is repeated within the cycle (revolution) τ_c considered and within the entire set of cycles prescribed.

Examples of Investigations. Examples of concrete comprehensive investigations of the dynamic and quasistationary operating conditions of continuous-operation generators of gas-turbine plants, carried out by the program based on the above-described mathematical model and algorithm, will be given in the second part of our work. Examples of investigations of an atmospheric-pressure regenerator with a matrix packed with various bodies and an intermediate gas-turbine plant regenerator are given in [29, 30].

The data of calculations of the parameters of regenerators with matrices of four types by the mathematical model and program developed by us and the known data of other authors [2, 5, 21, 23] obtained with the use of different quasistationary, classical analytical models are presented in Table 1. The examples were selected strictly by the completeness of the initial data presented; however, some of the data [5, 21] have to be determined or recalculated. In our investigations carried out with the use of the above-described nonlinear, distributed mathematical model based on the calculation of the local heat-transfer coefficients and aerodynamic drags by the above-indicated empirical dependences, we tried to most closely comply with the formulation of the problem given by the authors of the data compared. For the regenerators considered in [5] and [21], the thermophysical properties of the heat-transfer agents were

determined by the polynomial approximations involved in the program, since the corresponding data of the authors of these works are incomplete [5] or are absent [21]. Any correction factors were not introduced.

A comparison of the data, given at the bottom of Table 1, where they are separated by an additional line, shows that the data of our calculations of the design characteristics (heating surface, matrix mass) and parameters (heat-transfer coefficient, aerodynamic drag, degree of regeneration) of the regenerators considered are in satisfactory agreement with the corresponding data of other authors. It should be noted that the heat balance was calculated with a high degree of accuracy for the prescribed limiting rotational speed of the rotor in the case of heating from the cold state. This comparison of the data obtained with the use of the mathematical model proposed with the data obtained with simplified analytical quasistationary models, carried out with an example of not very complex calculations, can be considered as a good verification of this model.

CONCLUSIONS

A nonlinear, variable model based on the system of equations of mass and energy transfer in heat-transfer agents and the equation of heat conduction in a two-dimensional matrix wall has been developed for investigating the heat and aerodynamic processes in regenerative heat exchangers of continuous and periodic operation. Finite-difference schemes of equations and a convenient numerical algorithm based on successive runs-through in the directions longitudinal and transverse with respect to the flow, which eliminates global iterations in solving the conjugate problem of nonstationary heat exchange and allows one to calculate the heat balance with a high degree of accuracy, are proposed. A satisfactory agreement of the data of our calculations of the design characteristics and all the main parameters of the regenerators considered with the corresponding data of other authors has been demonstrated with an example of not very complex calculations that can be done with the use of classical, analytical quasistationary models, which is evidence of the correctness of the basic notions used in the model proposed.

NOTATION

A, *B*, linear coefficients for the heat-conduction equation; *a*, *b*, *C*, sets of "grid" parameters; *c*, heat capacity, J/(kg·K); $d = 4S/P$, hydraulic diameter of the channel, m; *E*, run-through coefficient for the heat-conduction equation; *f*, set of grid parameters; *G*, flow rate, kg/sec; Gz = Re Pr *d*/*L*, Graetz criterion; *h*, step of integration with respect to *x*, m; *I*, number of bands of integration with respect to *z*; *J*, number of bands of integration with respect to *y*; *k*, set of grid parameters; *L*, length of the channel, m; *M*, total number of grid points for the heat-conduction equation (numbering begins with 0); *m*, current number of a grid point for the heat-conduction equation; *N*, number of matrix-material layers; $Nu = \alpha d/\lambda$, Nusselt criterion; *n*, vector normal to the surface; $Pr = \mu c_p/\lambda$, Prandtl criterion; *p*, pressure, Pa; *Q*, heat flow, W; *q*, specific heat flow, W/m^2; *R*, gas or air constant; J/(kg·K); $Re = wd/\nu$, Reynolds criterion; *r*, radial coordinate, m; *S*, cross section of the channel, m^2; *t*, air temperature, ^{o}C; *U*, run-through coefficient for the heat-conduction equation; *w*, velocity of the flow in the channel (in the *z* direction), m/sec; *x*, generalized coordinate, m; *y*, coordinate perpendicular to the flow, m; *z*, coordinate parallel to the flow, m; α, heat-transfer coefficient, W/(m^2·K); β, γ, sets of grid parameters; Δ, difference or space step; Δp, pressure drop, Pa; Δy and Δz, steps of integration over the thickness and the length, m; $\Delta\tau$, step of integration with respect to time, sec; δ, calculated thickness of the channel wall, m; ε, degree of blackness; ζ, limited coefficient of friction; η, coefficient of heat efficiency; θ, temperature of the matrix wall, ^{o}C; ϑ, temperature of the gas, ^{o}C; λ, heat-conduction coefficient, W/(m·K); μ, dynamic viscosity, Pa·sec; $\nu = \mu/\rho$, kinematic viscosity, m^2/sec; Π, perimeter of the channel, m; π, index of a coordinate axis; ρ, density, kg/m^3; σ, approximation parameter of a scheme; σ_0, Boltzmann constant; τ, time, sec; φ, angular coordinate. Subscripts: abs, absolute temperature scale; a, air; inp, input; out, output; g, gas; b, boundary; ray, radiation; m, matrix material; l.d, local drag; in, initial; in.c, initial condition; end, end; r, reduced; av, average; f, friction; p, packing; c, cycle; *I*, number of the end point on the *z* coordinate; *i*, number of a point on the *z* coordinate; *J*, number of the end point on the *y* coordinate; *j*, number of a point on the *y* coordinate; *l*, number of a matrix-material layer; *M*, number of the end point for the heat-conduction equation; *m*, number of the current point for the heat-conduction equation; *p*, constant pressure; *v*, constant volume; π, current coordinate axis; Σ, summarized value; *n*, number of a time step; max, maximum; ch, channel; 1, individual channel; $\pm 1/2$, values averaged over a band; overscribed bar, average integral value; *, predicted value; plus (+), to the right of a point; minus (–), to the left of a point.

REFERENCES

1. H. Hausen, *Heat Transfer in Counterflow, Parallel Flow and Cross Flow*, 2nd ed., McGraw-Hill, New York (1983).
2. F. W. Schmidt and A. J. Willmott, *Thermal Energy Storage and Regeneration*, Hemisphere, McGraw-Hill, Washington, DC (1981).
3. R. K. Shah and D. P. Sekulic, Heat exchangers, in: W. M. Rohsenow, J. P. Hartnett, and Y. I. Cho (Eds.), *Handbook of Heat Transfer*, Ch. 17, 3rd ed., McGraw-Hill (1998), pp. 1–169.
4. R. A. Johnson, The AGT 100. Allison gas turbine operations General Motors Corp. Indianapolis, *Ind. Mech. Eng.*, May (1984), 36–43.
5. V. K. Migai, V. S. Nazarenko, I. F. Novozhilov, and T. S. Dobryakov, *Regenerative Rotary Air Heaters* [in Russian], Energiya, Leningrad (1971).
6. V. A. Krivandin, I. N. Nevedomskaya, V. V. Kobakhidze, et al., *Metallurgical Thermal Engineering. Vol. 2. Design and Operation of Furnaces* [in Russian], Metallurgiya, Moscow (1986).
7. I. I. Pereletov, L. A. Brovkin, Yu. I. Rozengart, et al., *High-Temperature Heat-Technology Processes and Installations* [in Russian], Energoatomizdat, Moscow (1989).
8. W. Nusselt, Die Theorie des Winderhitzers, *VDI-Zeitung*, **71**, 85–91 (1927).
9. A. Hill and A. J. Willmott, Modelling the temperature dependence of thermophysical properties in a closed method for regenerative heat exchanger simulations, *Proc. Inst. Mech. Eng.*, **202**, 195–206 (1991).
10. R. Scaricabarozzi, Simple particular solutions and speed calculation of regenerators, *Heat Recovery Syst.*, CHP, **9**, 421–432 (1989).
11. D. R. Atthey, An approximate thermal analysis for a regenerative heat exchanger, *Int. J. Heat Mass Transfer*, **31**, 1431–1441 (1989).
12. F. de Monte, Cyclic steady thermal response of rapidly switched fixed-bed heat regenerators in counterflow, *Int. J. Heat Mass Transfer*, **42**, 2591–2604 (1999).
13. H. Klein and G. Eigenberger, Approximate solutions for metallic regenerative heat exchangers, *Int. J. Heat Mass Transfer*, **44**, 3553–3563 (2001).
14. G. D. Bachnke and C. P. Howard, The effect of longitudinal heat conduction on periodic flow heat exchanger performance, *ASME J. Eng. Power*, **86**, 105–120 (1964).
15. R. K. Shah, A correlation for longitudinal heat conduction effects in periodic flow heat exchanger, *ASME J. Eng. Power*, **97**, 453–454 (1975).
16. A. J. Willmott, The regenerative heat exchanger computer representation, *Int. J. Heat Mass Transfer*, **12**, 997–1013 (1969).
17. P. J. Heggs, L. S. Bansal, R. S. Bond, and V. Vazakas, Thermal regenerator design charts including intraconduction effects, *Trans. Inst. Chem. Eng.*, **58**, 265–270 (1980).
18. C. M. Chen and W. M. Worek, The effect of wall conduction on the performance of regenerative heat exchangers, *Energy*, **17**, 1199–1213 (1992).
19. A. J. Willmott and C. Hinchcliffe, The effect of gas heat storage regenerator calculations, *Int. J. Heat Mass Transfer*, **19**, 821–826 (1976).
20. Ren Zepei and Wang Siyong, A theoretical and experimental investigation of heat transfer performance of rotary regenerative heat exchanger, in: *Proc. Int. Symp. on Heat Transfer*, October 15–18, 1985, Tsinghua University (1985), pp. 89–97.
21. R. K. Shah and T. Skiepko, Influence of leakage distribution on the thermal performance of a rotary regenerator, *Appl. Thermal Eng.*, **19**, 685–705 (1999).
22. M. A. Ebadian and Z. F. Dong, Forced convection, internal flow in ducts, in: W. M. Rohsenow, J. P. Hartnett, and Y. I. Cho (Eds.), *Handbook of Heat Transfer*, Ch. 5, 3rd ed., McGraw-Hill, (1998), pp. 1–137.
23. W. M. Kays and A. L. London, *Compact Heat Exchangers*, 3rd ed., McGraw-Hill (1984).
24. I. E. Idel'chik, *Handbook on Hydraulic Resistance* [in Russian], Mashinostroenie, Moscow (1975).
25. G. I. Marchuk, *Methods of Computational Mathematics* [in Russian], Nauka, Moscow (1989).

26. V. M. Paskonov, V. I. Polezhaev, and L. A. Chudov, *Numerical Simulation of Heat and Mass Transfer Processes* [in Russian], Nauka, Moscow (1984).
27. V. P. Kovalevskii, Calculation of nonstationary temperature fields of complex bodies of revolution in the presence of a nonideal thermal contact between composing materials, *Inzh.-Fiz. Zh.*, **40**, No. 5, 925–926 (1981).
28. M. B. Pozin, V. P. Kovalevskii, and A. V. Sudarev, A numerical conjugate distributed nonlinear mathematical model of periodically operating regenerators with a moving matrix, in: *Coll. of Sci. Papers of All-Russia Sci.-Res. Technol. Inst. of Power Energy Mech. Eng.* [in Russian], Nedra, Leningrad (1992), pp. 222–230.
29. V. P. Kovalevskii and S. Y. Kim, Numerical study of thermal and aerodynamic processes of an air-cooled regenerator of inert gases, *Tyazh. Mashinostr.*, No. 2, 5–10 (2003).
30. I. S. Yoo, V. P. Kovalevski, and S. Y. Kim, Numerical investigation of flowing processes for regenerators of transport gas turbine units, in: *Proc. Inst. Mech. Eng., Part A, J. Power Energy*, **217**, No. 3, 299–309 (2003).